

Supplemental information for

Increasing the sensitivity of micro X-ray fluorescence spectroscopy through an optimized adaptation of polycapillary lenses to a liquid metal jet source

Leona J. Bauer, Richard Gnewkow, Frank Förste, Daniel Grötzsch, Semfira Bjeoumikhova, Birgit Kanngießner and Ioanna Mantouvalou

S1. Consideration of absorption effects when changing the electron beam width

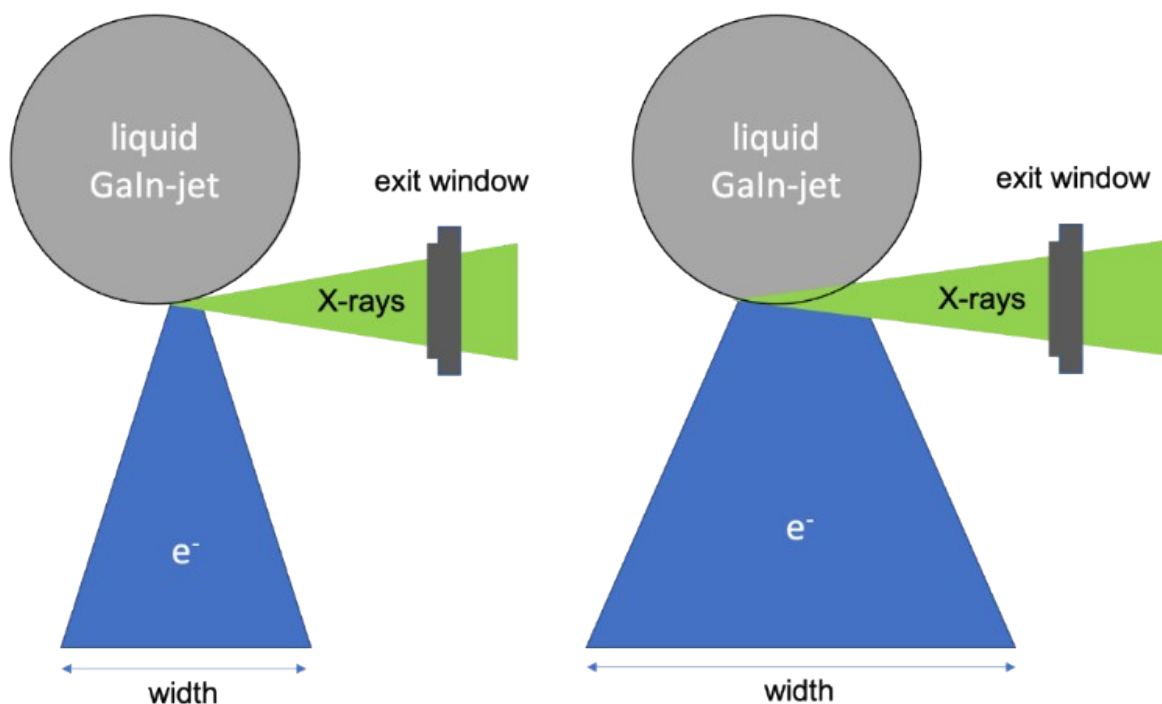


Figure S1: Schematic top-view of the liquid metal jet chamber. Shown are two different widths of the electron beam, which is not centered on the metal jet, but shifted in direction to the exit window, and the emitted X-ray radiation, which passes through the exit window.

By increasing the beam width, the part of the emitted X-ray radiation (schematically the green area within the black circle) which is attenuated on the way to the exit window increases and therewith the intensity of the excitation spectrum decreases.

S2. Gumbel function

Table S1: Gumbel function parameters and their uncertainties derived from fluorescence measurements.

Lens nr.	A	+/-	w	+/-	E_c	+/-
A: 280mls19	0.095	0.02	2.1	0.6	10.4	0.4
B: 250mls03	0.11	0.02	2.7	0.7	11.1	0.3
C: 244mkl41	0.08	0.02	2.5	0.8	11.0	0.3
D: 231mls25	0.13	0.04	3	1	11.9	0.5

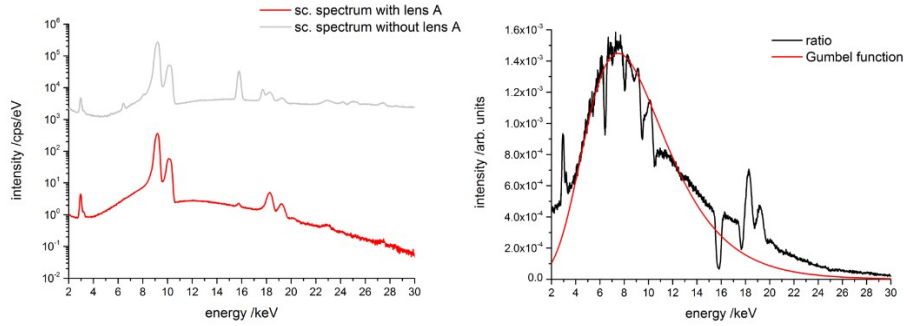


Figure S2: Scattering measurements to derive the Gumbel function. (Left) The measured scattered spectra with and without lens (A). The spectrum measured without lens is divided by the solid angle defined by the aperture of the sample holder. (Right) In black the ratio between the scattered excitation spectrum with and without lens is shown. In red the fitted Gumbel function is shown.

S3. Focal spot size by varying source size – SEM like and micro lens

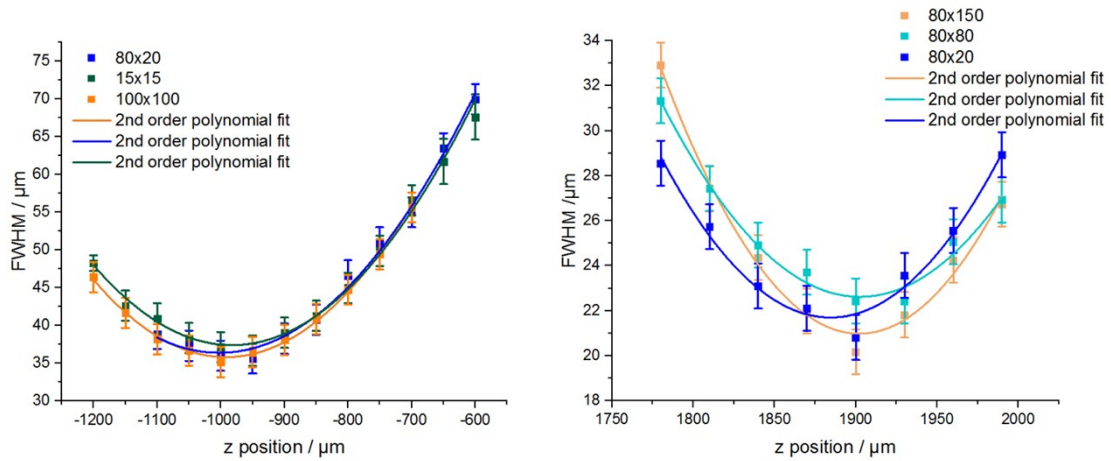


Figure S3: FWHM values for Fe K_{α} derived from knife edge scans on a razor blade in fluorescence mode for several positions along the x-ray beam focused by the polycapillary optics - SEM like lens (left) and the micro lens (right) - using different source spot sizes. The measurement points were fitted by a second order polynomial.

S4. Element distributions of P K, S K, Cl K and Br K.

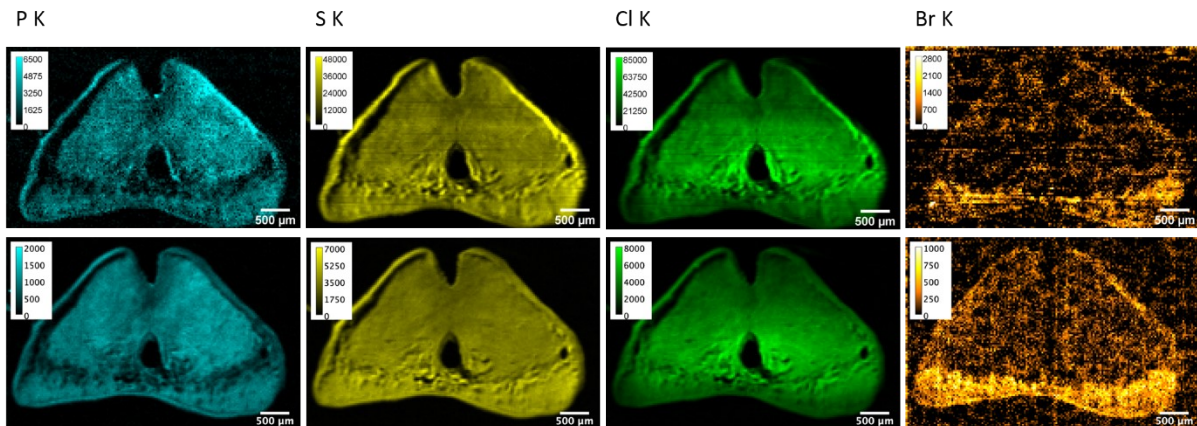


Figure S4: Net peak intensity distributions derived from μ XRF measurements collected with the LMJS setup (top row) and the M4 Tornado (bottom row). The net peak intensity distributions measured with the LMJS setup are corrected using the correction procedure described in section S5. The color bars which are optimized for best image contrast give the measured intensities in counts per second (CPS) per steradian (sr) of the fluorescence signal.

S5. Correction procedure of μ XRF measurement with the LMJS on mussel foot cross section

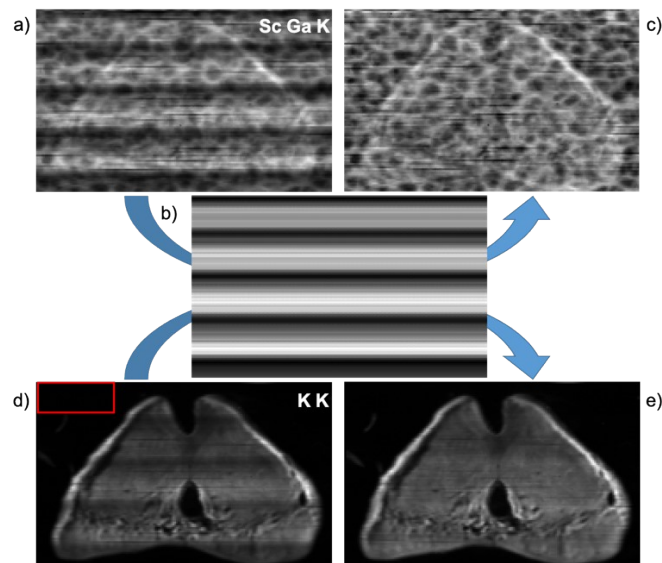


Figure S5: Schematic correction procedure of intensity distributions derived by μ XRF measurements on the mussel foot cross section with the LMJS.

Due to excitation intensity fluctuations caused by temperature variations during the measurement, the element distributions measured with the LMJS setup need to be corrected using the scattered signal. The measured scattered Ga K intensity distribution (Figure S5a) is used to create a same sized image, where every row consists of the mean value of the measured intensities in the respective row (Figure S5b). For the correction of the measured intensities, the scattered signal as well as the net peak intensities of the element distributions are divided with the generated mean value image (Figure S5b) using the 'Image calculator' function in 'Image J' (version 2.1.0/1.53c). In Figure S5c and S5e, the corrected scattered image and the corrected K K distribution are depicted. The only difference between the correction procedure of the scattering image and the element distributions is, that for the latter also the background is corrected. Therefore, the mean background value from the rectangle marked in Figure S5d was subtracted from the intensity value in every pixel.